An Oligomeric Equilibrium Intermediate as the Precursory Nucleus of Globular and Fibrillar Supramacromolecular Assemblies in a PDZ Domain

Javier Murciano-Calles,[†] Eva S. Cobos,[†] Pedro L. Mateo,[†] Ana Camara-Artigas,[‡] and Jose C. Martinez[†]*
[†]Department of Physical Chemistry and Institute of Biotechnology, Faculty of Sciences, University of Granada, Granada, Spain; and [‡]Department of Physical Chemistry, Biochemistry and Inorganic Chemistry, Faculty of Experimental Sciences, University of Almeria, Almeria, Spain

ABSTRACT The equilibrium unfolding at neutral pH of the third PDZ domain of PSD95, as followed by DSC, is characterized by the presence of an equilibrium intermediate with clear signs of oligomerization. DLS and SEC measurements indicate that at 60–70°C small oligomers populate, showing a typical β-sheet far-UV CD spectrum. These intermediate species lead to the formation of rodlike particulates of ~12 nm, which remain in solution after 2 weeks incubation and grow until they adopt annular/spherical shapes of ~50 nm and protofibrils, which are subsequently fully transformed into fibrils. The fibrils can also disaggregate after the addition of 1:1 buffer dilution followed by cooling to room temperature, thus returning to the initial monomeric state. Growth kinetics, as shown by ThT and ANS fluorescence, show that the organization of the different supramacromolecular structures comes from a common nucleation unit, the small oligomers, which organize themselves before reaching the incubation temperature of 60°C. Our experiments point toward the existence of a well-defined reversible, stepwise, and downhill organization of the processes involved in the association-dissociation of the intermediate. We estimate the enthalpy change accompanying the association-dissociation equilibria to be 130 kJ $\times$ mol^{-1}. Furthermore, the coalescence under essentially reversible conditions of different kinds of supramacromolecular assemblies renders this protein system highly interesting for biophysical studies aimed at our further understanding of amyloid pathological conditions.

INTRODUCTION

PDZ domains constitute the most abundant protein interaction modules in mammals, where they have been identified as the main structural component of a variety of the so-called hub proteins. These highly connected protein-nodes may have hundreds of links, either simultaneously or sequentially, suggesting that hubs organize the proteome by acting as molecular engines that connect biological processes. As far as the PSD95 belonging to the MAGUK family, is concerned, its three PDZ domains, together with a SH3 domain and a guanylate kinase module, are involved in the complex process of synapse scaffolding (1). It is surprising that only five functional domains might be responsible for the organization of the dynamic trafficking of a variety of synaptic proteins at the inner face of the neuron membrane. The explanation may well be that the intrinsic structural plasticity of hub proteins derives from the corresponding plasticity of their domains and linker sequences, which are able to explore the conformational space to discover the different strategies necessary to develop their various functions. In this way, the correlation between folding (stability) and binding (peptide dissociation rate) parameters shown recently for the PTPBL-PDZ2 domain strongly suggests that these domains may depend on their stability and dynamics to develop their function (2).

A computational and mutational study has shown that an evolutionarily conserved network of interacting residues exists in the PSD95-PDZ3 domain, which may work as a communication pathway between distal parts of the molecule (3). Nevertheless, there is little evidence, if any, of a conformational transition on binding that might be associated with a functional allosteric network in PDZ3, the process being a pure lock-key mechanism (4,5). In addition, the few equilibrium-unfolding experiments carried out with PDZ domains (including PDZ3) using spectroscopic probes have shown a single transition that can be described by the two-state model (2,6). Given their presumable functional flexibility and their relatively greater size (>100 amino acids) compared to the small, two-state, globular proteins studied to date, it would be unlikely that these domains do not contain any marginally stable conformations under equilibrium conditions.

Thus we decided to study the folding behavior of the PSD95-PDZ3 domain at neutral pH in far greater depth by using calorimetric and spectroscopic information. Contrary to previous evidence, our DSC experiments show two unfolding transitions, which undoubtedly indicate the existence

Submitted November 30, 2009, and accepted for publication April 1, 2010.

*Correspondence: jcmh@ugr.es

Abbreviations used: ANS, 1-anilino-naphtalene-8-sulfonic acid; CD, circular dichroism; DLS, dynamic light scattering; DSC, differential scanning calorimetry; MAGUK, membrane-associated guanylate kinase; PDZ, postsynaptic density-95 protein, disk-large tumor suppressor protein, zonula occludens-1; PSD95, postsynaptic density-95 protein; PSD95-PDZ3 or PDZ3, third PDZ domain of PSD95 protein; PTPBL-PDZ2, second PDZ domain of protein tyrosine phosphatase-BL; SEC, size-exclusion chromatography; SH3, Src-homology 3 domain; TEM, transmission electron microscopy; ThT, thioflavine T; UV, ultraviolet.

Editor: Jane Clarke.

0006-3495/10/07/0263/10 $2.00

doi: 10.1016/j.bpj.2010.04.003

of at least three well-defined macroscopic states on unfolding. Moreover, the endotherms tend to separate along the T axis concomitantly with an increase in protein concentration, suggesting some degree of association of the intermediate state. The characterization of the size distribution of these oligomerization phenomena by DLS, SEC, and TEM shows that the monomeric native state partially unfolds on heating, thus generating small oligomeric species that lead firstly to disklike assemblies and protofibrils, and then to amyloid fibrils after incubation on various days at 60°C. A further conformational analysis of the intermediate state shows a high content of β-sheet structure as well as the absence of any lag-phase in time-dependent ThT and ANS fluorescence measurements.

The occurrence of globular and fibrillar arrangements in PDZ3 (simultaneous at some stages) may help to answer some crucial questions within this field of inquiry, which is of key interest toward our understanding of amyloid-generating pathologies and the development of effective therapies against them. So far, increasing evidence suggests that soluble oligomeric intermediates, rather than fully formed fibrils, are likely to be the primary toxic species, fibrillar aggregates being merely a storage or even protective mechanism (7). Within this context, cell degeneration and pathophysiology may derive from the organization of pores in membranes by such oligomers, most probably by specific ionic transport via ion channels, which would destabilize ionic homeostasis in vivo (8–10).

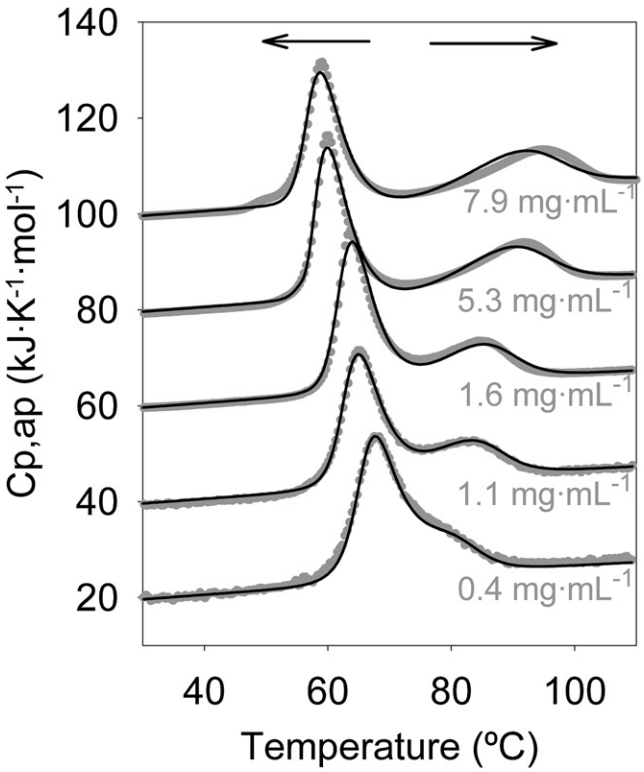

FIGURE 1 Thermal unfolding profiles of PSD95-PDZ3 monitored by DSC as a function of protein concentration. Experimental conditions were 50 mM K-phosphate, pH 7.5. The best fitting to the $N \rightleftarrows I_n \rightleftarrows U$ model is shown as black solid lines through the experimental data (*gray symbols*).

RESULTS

PDS95-PDZ3 thermal unfolding shows the population of an oligomeric equilibrium intermediate at neutral pH

The few equilibrium unfolding studies carried out to date using spectroscopic probes (fluorescence and CD) show that PDZ domains display a single sigmoid transition on both thermal and chemical denaturation. This behavior has been analyzed by using a two-state folding mechanism (6,11–13). We have measured the CD thermal unfolding of PSD95-PDZ3 in 50 mM K-phosphate buffer at pH 7.5 and been able to corroborate this behavior (data not shown). Nevertheless, nothing can be concluded at this juncture, as will be shown below.

Among the variety of biophysical techniques available, DSC would seem to be the best choice to detect any equilibrium conformation(s) that might be populated during unfolding. In this thermodynamic study, in what we believe to be the first reported for a PDZ domain to date, we have explored the unfolding of PSD95-PDZ3 in 50 mM K-phosphate buffer at pH 7.5 (Fig. 1). Protein preparation and experimental details are described in the Materials and Methods section in the Supporting Material. The thermal unfolding profiles were partly reversible during the timescale of the DSC experiments (at least 60%) and the scan rate did not affect their shape in any appreciable way (data not shown). The reversibility of some heat-denatured solutions was further checked by far-UV CD spectrum analysis, which showed that the complete N-state spectrum can be arrived at after a few hours. These features indicate clearly the slow relaxation times of these association phenomena but do not contradict their equilibrium nature at neutral pH.

Despite the evidence of the spectroscopic probes, however, the two unfolding transitions observed in Fig. 1 for all protein concentrations undoubtedly indicate the existence of not less than three well-defined macroscopic states during unfolding. Furthermore, both endotherms distance themselves from each other along the T axis concomitantly with an increase in protein concentration, suggesting some degree of association of the intermediate state. Thus, the movement of the first transition to lower temperatures (corresponding to the $N \rightleftarrows I$ equilibrium) indicates an increase in the association stage of the final I-state during unfolding, whereas the opposite is true for the second transition (corresponding to the $I \rightleftarrows U$ equilibrium). The effect of protein concentration on DSC traces has been described elsewhere in some other examples and is a consequence of the increase in population of the associated species concomitant with protein concentration (14,15). This characteristic

behavior may in fact explain the apparent single-transition two-state behavior observed previously because at the low PDZ3 concentrations used in spectroscopic thermal unfolding experiments the associated intermediate does not populate significantly enough to be observed. Thus it can be seen in Fig. 1 that the behavior of the DSC trace at 0.4 mg $\times$ mL^{-1} is more that of a single-transition than those obtained at higher protein concentrations, where both endothermic effects are well distinguished. In short, PDZ3 unfolding can be summarized by the equilibrium scheme

$$nN \rightleftarrows I_n \rightleftarrows nU. \qquad \text{(Scheme 1)}$$

This model fully describes the experimental unfolding behavior of PDZ3, as will be explained in the following sections.

The oligomeric intermediate can lead to the reversible organization of annular/spherical and fibrillar aggregates at neutral pH

To characterize the postulated association-dissociation equilibria we undertook DLS experiments as a function of temperature (Fig. S1). A PDZ3 solution at a concentration of 8 mg $\times$ mL^{-1} in 50 mM K-phosphate pH 7.5 was heated initially from 20 to 60°C, which is the maximum operating temperature of the instrument and high enough to ensure that the I_n species should be most populated according to DSC analysis (see next section). The temperature was then kept at 60°C, at which moment the mass evolution of the species (raw relative intensity) as a function of incubation time was recorded (Fig. S1). Finally, the protein sample was cooled down inside the instrument to 20°C. A summary of the spectra obtained at different times after reaching this temperature is set out in Fig. S1.

As can be seen in Fig. S1, at low temperature the size distribution approaches that of a monomer (R_h = 1.8 nm). Nevertheless, at 60°C the size increases until reaching that corresponding to trimeric species (R_h = 2.6 nm) when analyzed according to the globular protein model provided by the software of the instrument. Some other heavier particles (R_h = 12 nm) also appear and become the major components of the solution after ~2 h incubation (Fig. S1). These particles, each containing ~100 monomers, increase in size when incubated for longer periods. Finally, on cooling the protein to 20°C, the 12 nm species appears once more in solution, as do the monomeric state and the far-UV CD spectra of the *N*-state after a few hours (Fig. S1). All these features support the reversible nature of these association reactions.

We incubated PDZ3 samples for longer periods of time at 60°C, during which the formation of supramacromolecular structures was followed by TEM imaging. In Fig. 2 we show a history of the evolution of such assemblies over time. In accordance with the DLS evidence, a background of rodlike particles of ~10–20 nm can be seen at the beginning (Fig. 2 *A*) and remain in the incubated solution for various days, growing to ~50 nm (Fig. 2, *C* and *D*). It is difficult to discern from TEM images what the true tridimensional shape of the globular aggregates might be; they may be considered to be either roughly annular, as can be deduced from the darkening of the circles toward the center (Fig. 2 *D*, *inset*), or possibly spheres, although in this case the darkening of the particles should be in the opposite direction. These globular particles coexist with other assemblies such as protofibrils (Fig. 2 *B*) and, eventually, a few large, thin fibrils can be made out (Fig. 2, *A* and *E*). The images taken over periods >15 days show only fibrillar structures (Fig. 2 *G*).

The final arrangement of the fibrils also seems to coexist reversibly with circular formations, because they disappear from the solutions incubated for 1 month on diluting 1:1 with buffer and cooling to room temperature, which

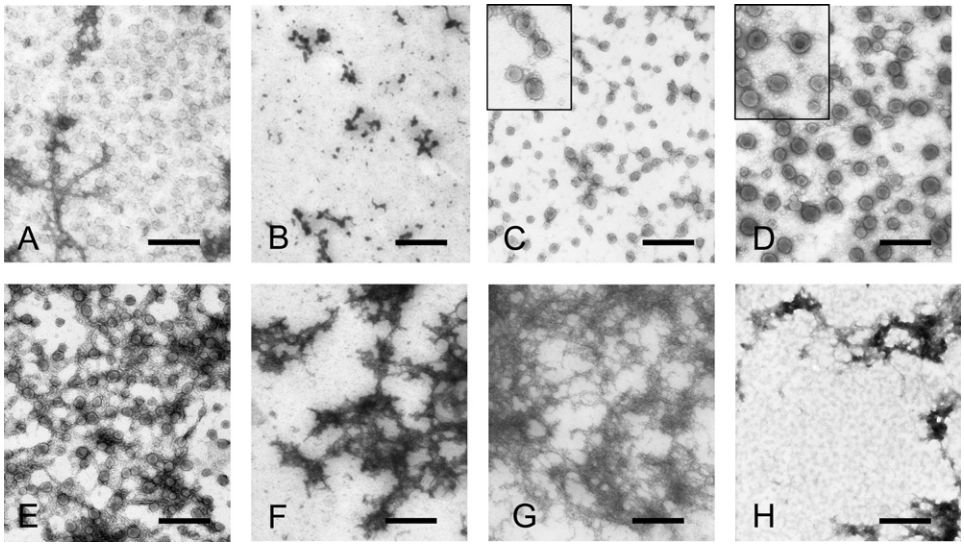

FIGURE 2 Transmission microscope analysis of PSD95-PDZ3 supramacromolecular assemblies. From left to right we show the globular particles obtained after (*A*) 3 and (*B*) 5 days incubation of the PDZ3 sample (8 mg $\times$ mL^{-1}) at 60°C and pH 7.5, the globular species and thin fibrils after (*C*) 8 and (*D–F*) 15 days, and (*G*) the fibrils that appear after 1 month. (*H*) Microaggregates seen after ~15 h reincubation of a 1:1 buffer-dilution on a 1-month-old sample. The scale bar corresponds to a size of 200 nm. The insets in the *C* and *D* are an enlargement of some of the globular motifs.

accelerates the disaggregation of the fibrils to within a few minutes. In addition, the background of 12 nm rodlike structures appeared again when the diluted samples were reincubated at 60°C for ~15 h (Fig. 2 *H*). Whatever the case, the essentially reversible character of this process does not seem to be 100%, because some aggregates remain in the solution after dilution (Fig. 2 *H*). It may be that irreversibility increases concomitantly with the size of the fibrils and ageing, as has been reported elsewhere for other examples (16).

In summary, it seems that the oligomeric equilibrium intermediate organizes itself into a set of globular particles and protofibrils at the early stages of the incubation reaction and that these persist for 2 weeks incubation, after which they all become fibrillar. The most interesting feature that emerges from DLS and TEM imaging is definitely the coexistence in a reversible fashion of both fibrils and annular/spherical arrangements in the same PDZ3-incubated solution at neutral pH. The images taken after a few days incubation at 60–70°C show that some thin protofibrils seem to appear (Fig. 2 *B*), in some cases as though they were emerging from the surfaces of the globular species (Fig. 2 *E*), perhaps growing at the expense of the latter because we could not find any trace of circular-shaped particles within the oldest incubated samples. A further imaging analysis using more powerful instruments is needed to settle these matters.

Insights toward energetic and conformational aspects of the oligomeric intermediate through the equilibrium analysis of PSD95-PDZ3 unfolding

We carried out some fitting sessions of DSC experiments using the three-state association-dissociation model (Scheme 1), as described in Materials and Methods in the Supporting Material. The DLS results (Fig. S1) indicate that the degree of association of the I_n-state can be globally assumed as $n = 3$ because during the initial 20 min of incubation at 60°C most of the species had an average hydrodynamic radius of 2.6 nm, which is close to the corresponding molecular size of trimeric species (33 kDa). This period roughly reflects the time that the protein sample remains at these high temperatures inside the DSC cell because the instrument is usually operated at scan rates ranging between 1–2°/min. As can be seen in Fig. 1, the quality of the nonlinear curve fitting of the calorimetric traces leads us to conclude that the model fully describes the experimental unfolding behavior of PSD95-PDZ3.

DSC experiments have also been fitted to the model, keeping the value of n free to float. The results of this fitting session give a value of $n = 3.8 \pm 0.3$ and also the best R- and R^2-values (0.996; Fig. S2). Correspondingly, as shown in Fig. S2, the fitting with a fixed value of $n = 4$ meets the convergence criteria somewhat better than the one with $n = 3$. There are some small deviations in the second endotherms of traces at high protein concentrations, but the fitting with $n = 3$ reproduces the shape of the trace at 0.4 mg $\times$ mL^{-1} more satisfactorily. The use of other values for n, from 2 to 6, resulted in worse fittings (Fig. S2). The explanation of these features might be that as protein concentration increases the larger species become more populated concomitantly with the stabilization of the intermediate state and thus their influence in DSC experiments is somewhat more noticeable. The thermodynamic parameters in Table 1 have been calculated from the fitting sessions using $n = 3$, where the error intervals have been estimated by comparing the parameters obtained at both $n = 3$ and $n = 4$ values. These errors are slightly higher and possibly more realistic values than fitting standard errors.

The dependence on concentration of DSC traces has been studied extensively in the past by different research groups, including ours (14,15). These studies have shown clearly that the relative displacement of traces obtained under the same solvent conditions can be exclusively attributed to protein concentration differences and, thus, the global stoichiometry of the association-dissociation process can be precisely obtained from the evaluation of such displacement through global fitting analysis of the whole set of traces (as we have done in this study), as long as the protein concentrations have been correctly measured for the set of experiments. We obtained additional evidence of these association phenomena from DLS and SEC experimental approaches (Fig. S1). As well as the DSC evidence, the DLS experiments carried out at low protein concentration (0.4 mg $\times$ mL^{-1}) do not show any significant population of aggregated species at any time of incubation at 60°C, which is further supported by the absence of any fluorescence enhancement of solutions incubated with ANS or ThT (data not shown).

The hypothetic trimeric nature of the oligomeric species is shared by other examples (8,17) and can be structurally understood here from a computational analysis of PDZ3 sequence propensity to β-aggregation. The calculations using the Tango algorithm developed by Fernandez-Escamilla et al. (18) show that propensities are negligible over

TABLE 1 Thermodynamic parameters of the thermal unfolding of the PSD95-PDZ3 domain in 50 mM K-phosphate pH 7.5 obtained from the analysis of DSC experiments

$T_{N\text{-}U}$ (°C)	$\Delta H_{N\text{-}U}(T_{N\text{-}U})$ (kJ $\times$ mol^{-1})	$\Delta G_{N\text{-}U}(298)$ (kJ $\times$ mol^{-1})	$T_{U\text{-}In}$ (°C)	$\Delta H_{U\text{-}In}(T_{U\text{-}In})$ (kJ $\times$ mol^{-1})	$\Delta G_{U\text{-}In}(343)$ (kJ $\times$ mol^{-1})
70.4 ± 0.5	335 ± 20	39 ± 6	79.2 ± 1.2	−130 ± 20	25 ± 5

The error intervals were calculated as described in the text. The values of thermodynamic magnitudes for the $U \rightleftarrows I_n$ equilibrium were estimated for a $P_{ref} =$ 100 μM. The heat capacity functions obtained from the fitting were $C_{pN} = -9.23 + (0.095*T)$; $C_{pU} = 2.91 + (0.064*T)$; $C_{pIn} = -99.0 + (0.347*T)$ in kJ $\times$ mol^{-1}.

the whole domain with the exception of residues ranging from 340 to 350 (pertaining to the β3 and α1 motifs) and for the 392–397 ones (located at β5 and α3 secondary structures). The tridimensional arrangement of these residues in the high-resolution x-ray structures, recently solved by us (PDB codes: 3K82 and 3I4W (19)), shows two main interfaces roughly located at opposite faces of the globular structure, which may allow each monomer to interact with two additional ones (Fig. S3). Thus, it is possible that the increase in solvent exposure of these aggregation-prone regions during unfolding may in PDZ3 monomers develop some tendency to self-associate.

In any case, we cannot rule out the idea that the experimentally observed oligomeric arrangement would result from a mixture of dimers, trimers, tetramers, or other oligomers, where the fraction of the lower-sized species decreases concomitantly with a decrease in protein concentration, which might be more probable from a mechanistic point of view. In fact, the coexistence of different association stages for these nucleation species has been reported for some other amyloid-forming proteins (20). The existence of such additional equilibria might also constitute an alternative explanation for the small DSC deviations observed in the fitting sessions and may contribute to some extent to the greater sharpness and asymmetry of the first endotherm (Fig. 1). To investigate these issues, we conducted SEC experiments at pH 7.5 and 60°C with 8 mg $\times$ mL^{-1} PDZ3 samples incubated for different periods of time (Fig. S1). A broad peak appears, probably due to the presence of a mixture of sizes, albeit the maximums observed correspond to monomers, high aggregates (at the exclusion volume) and, once again, roughly trimeric species.

To achieve a better understanding of the energetics of the intermediate state we dissected the two DSC endotherms (Fig. 1) into their respective heat contributions. To this end, we developed the equations corresponding to the model scheme described by Eq. 2 of the Supporting Material. This alternative scheme, mathematically equivalent to the one in Eq. 1 of the Supporting Material, allows us to obtain separately the contributions corresponding to the unfolding and association-dissociation processes, which may help to understand the unfolding process phenomenologically. Thus, the deconvolution analysis shown in Fig. 3 shows that the evolution of heat during the unfolding process occurs exclusively during the first endotherm ($N \rightleftarrows I_n$), which seems to be the result of the combination of two processes of opposite signature: the positive contribution of the whole heat of the protein unfolding process and the exothermic component deriving from the association phenomena of the intermediate state. Nevertheless, the second evolution can be attributed merely to the heat released by the disruption of interdomain interactions during the dissociation of I_n oligomers into monomeric molecules (Fig. 3 *B*), which does not necessarily include any other heat contribution deriving from the further unfolding of the intermediate. Consequently,

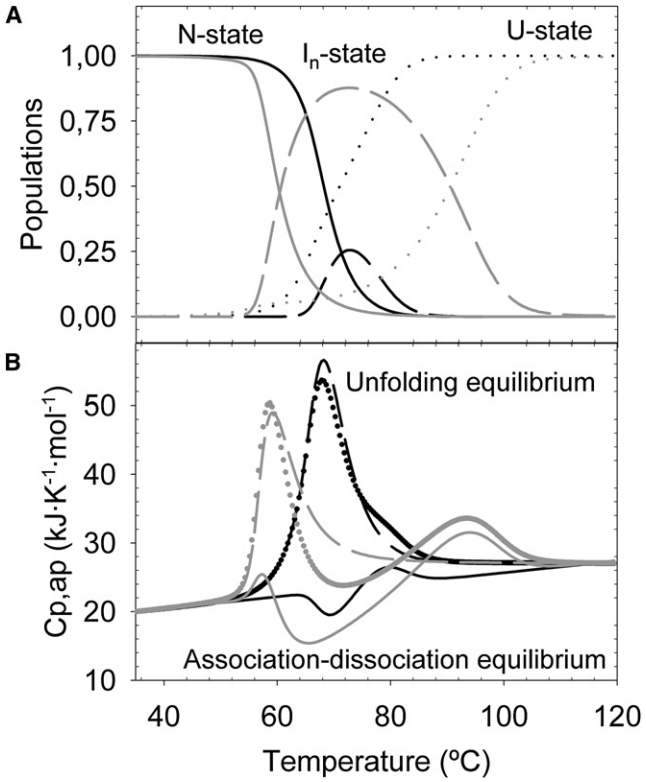

FIGURE 3 Deconvolution analysis of the different equilibria for PSD95-PDZ3 thermal unfolding. (*A*) Distribution of populations of the different PDZ3 states for the two extreme protein concentrations assayed, 0.4 mg $\times$ mL^{-1} (*black*) and 8 mg $\times$ mL^{-1} (*gray*). An increase in I_n-state population can be seen on protein concentration. (*B*) Dashed lines show the respective thermal evolutions of the unfolding equilibrium ($N \rightleftarrows U$) and the solid lines the association-dissociation term ($U \rightleftarrows I_n$). Symbols are used for experimental DSC data as a function of protein concentration. As can be seen, the latter equilibrium is symmetrical in shape because the intermediate associates first (exothermic half) and dissociates afterward (endothermic half) to complete unfolding.

these findings indicate that from an energetic point of view the I_n-state may resemble a partly unfolded state in which most of the tertiary cooperative interactions are relaxed, rather than a highly structured, cooperative, nativelike arrangement. The nonnative character of this partly folded state is also revealed by its incapability of recognizing the high-affinity PDZ3 ligand KKETAV, which in no way influences the history set out in Fig. 2.

Whatever the case, the high quality of the fittings (Fig. 1 and Fig. S2) cannot in itself be considered conclusive with regard to the completely noncooperative character of the unfolding of this intermediate and so we cannot definitely rule out the existence of more-or-less well ordered regions in this state. The oligomers may possibly maintain some local structural arrangements or perhaps contain new structural elements not present in the native state, and therefore this state may be considered as being partly folded even though it is not fully homogeneous. The SEC experiments (Fig. S1), for example, indicate that at 60°C monomeric

species of this intermediate state can be discerned, which supports the idea that it displays some thermodynamic stability by itself. The smallness of the structural arrangements will lead to a relatively small and rather wide heat effect.

Spectroscopic and kinetic analysis of the early conformational stages of the PDZ3 misfolding pathway

We investigated the structural ordering of the intermediate by far-UV CD spectroscopy. Fig. S4 includes the PDZ3 spectra at 25°C and 70°C, the two key temperatures for the *N*-state and the I_n-state respectively (Fig. 3 *A*). The spectrum at 70°C shows a high secondary-structure content for the associated states, which, according to the minimum observed at 217 nm, would be mainly β-sheet structures. These β-sheet organizations remained unaltered after several hours at this temperature. The absence of Trp residues, together with the low aromatic content within the hydrophobic core of PDZ3, prevented any further CD research into tertiary arrangements at the near-UV region.

Congo red and ThT dyes have been used traditionally as histochemical stains for amyloids (21). Both gave positive results when assayed with the mature amyloid fibrils of PDZ3, the former leading to a blue shift in the UV-visible spectrum (data not shown) and the latter to a noticeable enhancement of fluorescence signal (Fig. S5). Assays with the ANS fluorescent probe were also positive. This probe has been reported to bind solvent-exposed hydrophobic surfaces in proteins, producing an increase in fluorescence signal together with a blue shift in the maximum wavelength emission (Fig. S5), which indicate clearly the accumulation of partially structured species with solvent-exposed nonpolar surfaces.

To achieve some insight into the sequence of events that develop during the formation of PDZ3 fibrils we carried out a real-time continuous monitoring of the fluorescence signal from ThT and ANS (Fig. 4). The 8 mg × mL^{-1} PDZ3 sample was heated inside the fluorimeter to 60°C (Fig. 4 *A*) and, once at this temperature, the time-course of the fluorescence signal was monitored during the first few hours of the aggregation reaction at 60°C (Fig. 4 *B*). Finally, some fluorescence spectra were obtained after cooling the sample down to room temperature (Fig. S5). Thus, these time-course experiments paralleled the DLS ones described previously. When the PDZ3 sample was heated to >50°C some fluorescence signal was obtained for both dyes (Fig. 4 *A*). After setting the collection mode of the fluorimeter to time-dependent measurements at 60°C we found that at the very beginning both the ThT and ANS signals rose rapidly, reaching a clear maximum after 100 min with ThT and 400 min for ANS, and then decreasing. It might be surmised that the main reason for this decrease was the increase in light-scattering that parallels the greater viscosity

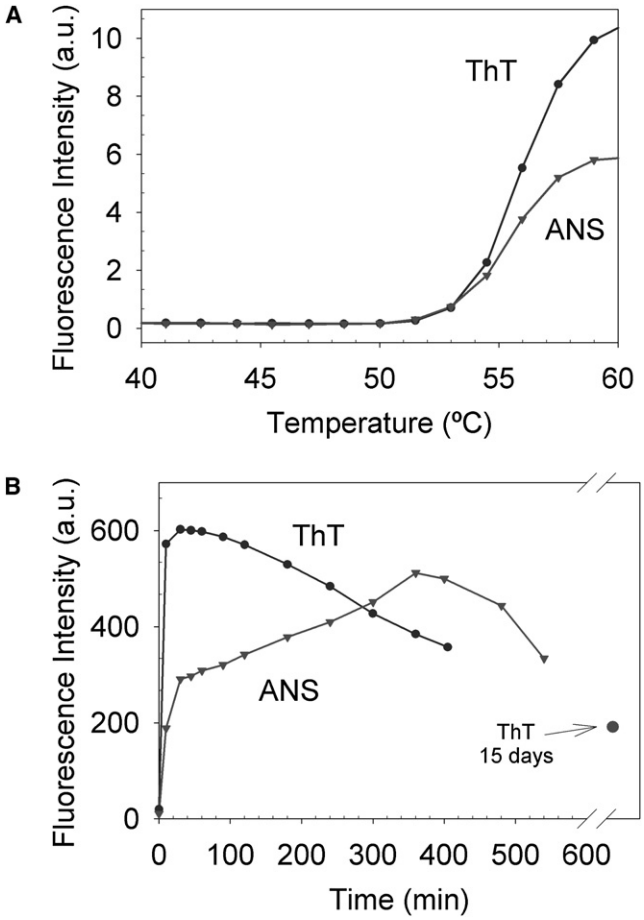

FIGURE 4 Growth kinetics of ThT and ANS fluorescence emission. A 8 mg × mL^{-1} PDZ3 sample was incubated in the presence of 12 μM of ThT or 20 μM ANS at pH 7.5. (*A*) Temperature dependence of fluorescence emission from both dyes. (*B*) Time dependence of the fluorescence signal versus incubation time at 60°C is plotted.

and turbidity of samples brought about by the insolubility of the supramacromolecular structures organized within this time (21–23). The protein samples became turbid and viscous and when the solutions were cooled to room temperature a hyper-chromic effect appeared as a consequence of the disaggregation of the assemblies into more soluble and lower molecular weight species (Fig. S5).

An interesting feature that emerges from Fig. 4 is the absence of the typical sigmoidal shape of the ThT and ANS curves obtained for the majority of examples studied previously (20,22,24). DLS measurements indicate that >50°C the monomers increase in size, to become practically 100% oligomeric at 60°C (Fig. S1). Accordingly, in Fig. 4 *A* it can be seen that the fluorescence signal of both probes begins to become temperature dependent at >50°C, which indicates clearly that the amyloid β-pleated structure identified by ThT fluorescence and the hydrophobic surface areas monitored by ANS fluorescence arose concurrently, as has been reported elsewhere for other examples (25). Thus, the formation of nuclei, held to be responsible for

the lag-phase of S-shaped curves, was complete before the sample's reaching the starting temperature. This would seem to indicate that under these experimental conditions nucleation is not a rate-limiting step for PDZ3 amyloid formation. Aggregation in these cases has been reported to proceed via a downhill process that does not require a highly organized or stable nucleus (20,26,27).

DISCUSSION

The PSD95-PDZ3 domain represents a typical medium-sized protein that unfolds via a multistate scheme

The thermodynamic parameters set out in Table 1 show that PDZ3 is a stable domain with an unfolding Gibbs energy of 40 kJ $\times$ mol^{-1}, which is comparable to the stability of other proteins of a similar size, such as barnase (28). This value does not compare well with the previous stability data obtained for PTPBL-PDZ2 or for PDZ3 itself, which ranges from 14 to 30 kJ $\times$ mol^{-1} (2,12). It is worth bearing in mind, however, that these previous results were obtained from a two-state analysis of spectroscopic unfolding data.

The oligomeric equilibrium intermediate detected in our experiments can be considered as a novel species not reported previously in other PDZ folding studies. Thus, the folding mechanism of several PDZ domains, including PSD95-PDZ3 itself, has been studied by folding kinetics. It can be described as having two transition states separated by a high-energy obligatory (on-pathway) intermediate. Both transition states are located at roughly the same positions along the reaction coordinate, indicating a conserved folding mechanism for PDZ domains. Nevertheless, despite the obligatory character of the intermediate, it never accumulates under equilibrium (2,13,29). An interesting NMR study has also been published on native-state hydrogen exchange using a longer construct of PDZ3, which identifies an equilibrium intermediate after the rate-limiting folding step (12). The structural ensemble of the intermediate closely resembles that of the native PDZ3 fold, with the exception of the first residues of the N-terminal tail, the third α-helix and a further β-hairpin organized by the C-terminal residues. Nevertheless, the PDZ3 sequence analyzed in our work, corresponding to residues 302–402 of the PSD95 protein, does not contain the β-hairpin sequence deriving from the cloning vector used in the work of Feng et al. and in other previous structural analyses (12). In any case, the additional evidence about the low cooperative folding character, the essentially β-sheet content and the oligomeric nature of the intermediate detected by DSC using the short PDZ3 construct makes this equilibrium intermediate substantially different from the one with the longer PDZ3 sequence, which is essentially nativelike (12).

We can only find one previous example in the DSC literature of a protein of a similar size to PDZ3 that also displays a monomeric α-β topology and has been studied according to the same equilibrium model, and that is the 14 kDa protein CheY (30). CheY and PDZ3 intermediates, as detected by DSC, share some common features, such as their tendency to associate themselves and their low unfolding cooperativity. Nevertheless, the organization of supramacromolecular structures in CheY has not yet been described. In any case, both PDZ3 and CheY firmly support the idea that medium-sized monomeric proteins (>~10 kDa) usually unfold in a more complex way than smaller ones and present at least one equilibrium intermediate.

Thermodynamic and conformational aspects of fibril organization on PSD95-PDZ3 unfolding

The formation of fibrils in PDZ domains has been reported very recently in the PTPBL-PDZ2 domain, as a result of a combination of mechanical stirring and high-ionic-strength solvents under native conditions at neutral pH. The combination of both forces, mechanical and electrostatic, leads to the appearance of amyloid fibrils in <24 h (6). Nevertheless, despite the native conditions of the solution, the fibrils show the typical CD and infrared spectra of pure β-sheet structures, as in the case of the PDZ3 unfolding intermediate.

Our studies with PDZ3 show some interesting features concerning the physical-chemical nature of processes involved in fibril organization. First, seeding may well occur through a β-sheet oligomeric nucleus, which suggests strongly a stepwise model for the organization of such large structures, as has been reported elsewhere for other examples (22,31,32). This nucleation phase is completed before temperature equilibration of PDZ3 samples, which results in a noncooperative (nonsigmoid) behavior of fibril growth (Fig. 4), in which the ensemble of critical oligomers adds to the different supramacromolecular assemblies in a downhill process (26,27,31). Second, the fibrils disaggregate after 1:1 dilution of the sample with a buffer solution at pH 7.5 and cooling to room temperature, and reform on heating again to 60°C. This evidence points to the reversible nature of processes involved in fibril formation despite their long relaxation times because they can disintegrate and rejoin spontaneously in a reversible manner. There are only a couple of other amyloid-forming proteins in which this phenomenon has been described: acylphosphatase (16) and apolipoprotein C-II (33). Therefore, PDZ3 fibrils offer an interesting and rare opportunity to study the disaggregation of these structural ensembles, which may help in the detection of new key species to explain the molecular nature of fibril formation and in the further development of treatments for diseases associated with protein aggregation.

From an energetic point of view, our work has also provided an unusual example of the thermodynamics of fibril formation. We have observed that the growth of oligomers does not seem to be accompanied by any conformational change in the intermediate state because the last DSC transition does not include any appreciable heat effects other than

that caused by the disaggregation of oligomers (Fig. 3 *B*). Accordingly, the far-UV CD spectra acquired as a function of time at 70°C do not show any apparent changes in shape (Fig. S4). A similar feature has been found in the previous calorimetric characterization of amyloid fibril formation in β_2-microglobulin (23) and in SH3 domains (24), which also display other similarities with PDZ3 that are worth mentioning. Thus, the enthalpy change of the dissociation of PDZ3 oligomers (-130 ± 20 kJ $\times$ mol^{-1}) coincides fairly closely with that corresponding to β_2-microglobulin (-125 kJ/mol^{-1}) and SH3 (-100 kJ $\times$ mol^{-1}) fibrils. These values are also in the range of those found for the dissociation of dimeric-equilibrium intermediates in CheY protein (30), which shares a common DSC-thermal unfolding behavior with PDZ3, as has been explained above. The quite small specific enthalpy value estimated for PDZ3 (11.8 J $\times$ g^{-1}) as well as for the other three examples indicates a relatively low density of side-chain packing interactions inside the fibrils. Whatever the case, all these enthalpic similarities argue in favor of entropic factors as being the driving force and point toward a similar energetic pathway for the organization of β-sheet stacking, as has also been suggested by the kinetic experiments (23,24).

In addition, the Gibbs energy at 70°C (the temperature at which these associated species populate according to Fig. 3) was 25 ± 5 kJ $\times$ mol^{-1}, whereas it was almost negligible at 25°C, where the stability of the native state has been estimated to be 40 ± 6 kJ $\times$ mol^{-1}. The greater stability of the native state than that of amyloid fibrils in PDZ3 may explain the reversibility observed between them because the native state is much preferred to the associated structures at room temperature. Accordingly, the contrary effect has been reported for the irreversible fibrils in β_2-microglobulin, where a higher stability value has been found for the fibrillar assemblies than for the *N*-state at any temperature (23). The stability of PDZ3 assemblies is clearly lower than that corresponding to β_2-microglobulin ones (44 kJ $\times$ mol^{-1}), which may indicate possible structural differences between them of entropic origin.

The PDZ3 unfolding scheme as a paradigm for the biophysical study of interconversion between supramacromolecular assemblies

The capacity to form amyloid fibrils is regarded today as a general property of all polypeptide chains. Less evidence exists concerning the formation of annular and spherical arrangements, but some recent and interesting work carried out by Quist et al. (8) has also shown that a set of unrelated amyloidogenic proteins and peptides display quite similar annular formations when assayed in the presence of reconstructed membranes, and are also able to act as ion transporters through them, i.e., as ion channels. This evidence also points clearly to a parallel ubiquitous nature for the formation of these species. The diameter of the channels ranges from 8 to 12 nm, similar to those reported here for the PDZ3 rodlike species of 12 nm (Fig. S1). A comparison of the different PDZ3 particulates also shows a relative homogeneity in their size (Fig. 2), which suggests that the organization of these arrangements is well-defined (8). Correspondingly, spherical aggregates ranging from 5 nm to 200 μm have been described, also pointing to their being a general property of polypeptide chains (34) and behaving as pore-forming species in lipid environments (35).

The relationship between annular/spherical species and amyloid fibrils has not been clearly determined. The question of whether there is a common pathway for the organization of these supramacromolecular structures or whether they are products of alternative misfolding pathways has remained unresolved until now, given the limitations of experimental systems (10). The majority of examples described shows a clear tendency to associate themselves in solution into small oligomeric species (generally from dimers to hexamers), although they can lead to disklike assemblies only in the presence of membranes (8). Alternatively, spheres usually organize under conditions close to the isoelectric point of the protein (34) and/or by adding organic solvents (35).

Interestingly, the PDZ3 globular arrangements can organize themselves in a membrane-free context, coexisting with the fibrils in the same buffered solution at neutral pH, lacking cosolvents or organic reagents. This rare phenomenon, together with the persistence of these globular assemblies in solution for at least 2 weeks, supports the view that they may be on-pathway, as has been proposed for human serum albumin (27), Sup35 (36), and Ure2p (32) proteins. In fact, as the TEM images show (Fig. 2), the fibrils grow at the expense of the globular arrangements, which disappear from the solution during the last stages of the incubation experiments. On the other hand, the concurrence of protofibrils during the early phases of the experiments, together with the fact that we could detect no globular assemblies in the 8 mg $\times$ mL^{-1} PDZ3 samples incubated at 37°C, only protofibrils and a few thin fibrils, does not allow us to arrive at any definitive conclusions about these matters (the TEM images obtained after 1 month incubation at 37°C were identical to those shown in Fig. 2 *B*).

The time experiments followed by DLS and ThT/ANS fluorescence provide additional information about these mechanistic matters because the absence of a nucleation phase (lag-phase) >50°C and the coincidence of the beginnings of the time-courses monitored by the different probes implies that a certain quantity of oligomeric ensembles displaying hydrophobic patches and β-sheet amyloidlike structures form concurrently after a common nucleation event. Something similar has been observed in the α-synuclein amyloidogenic protein. Consequently, we can also conclude that, if separate pathways exist (off-pathway mechanism), the branchpoint must be located after nucleation, i.e., after the I_n species in the PDZ3 folding scheme (37).

In summary, the experimental information can be summarized in the following scheme, intended to explain the unfolding behavior of the PSD95-PDZ3 domain in 50 mM K-phosphate at pH 7.5:

$$N \rightleftarrows I_n \rightleftarrows U$$
$$\downarrow\uparrow$$
GLOBULAR ASSEMBLIES AND PROTOFIBRILS
$$\downarrow\uparrow$$
FIBRILLAR ASSEMBLIES

(Scheme 2)

where the double arrows indicate the reversible nature of the different processes and not necessarily any true equilibrium situation, at least for the ones pertaining to the misfolding pathway. This folding behavior displayed by PDZ3 opens the possibility of entering more deeply into structural studies with the different supramacromolecular assemblies. CD experiments, together with ThT and ANS fluorescence emission, show that these structures have a high β-sheet content organized into amyloidlike structures that also expose a relatively high amount of hydrophobic surface to the solvent. In addition, the I_n-state cannot be considered as nativelike because it appears after a highly cooperative unfolding process from the native state, as shown by DSC, and neither is it able to recognize the high-affinity peptide KKETAV because its presence in the PDZ3-incubated solutions does not alter the temporal sequence of events given in Fig. 2.

Nevertheless, some other questions remain to be solved. It remains unclear, for example, how such oligomers can manage to organize themselves into defined ion-channel-like structures (10). Recent molecular dynamics simulations (38) have shown that in a membrane-free context double-layered annular structures exhibit high structural stability due to strong hydrophobic interactions and geometrical constraints induced by the closed-ring shape. These studies also reveal that annular structures can be postulated as an intermediate step in the aggregation pathway, leading to fibrils at later stages, which completely agrees with our PDZ3 experimental results. The quaternary structures contain two layers of β-sheet molecules stacked either parallel or antiparallel to the fibril axis, giving rise to disklike arrangements of 8–12 nm in diameter, with inner cavity pores of around 2 nm, which agrees with previous evidence (8) and our own experimental results.

The most recent studies indicate that fibrils could simply be a storage mechanism and that these smaller globular arrangements are sufficient to induce cell degradation by allowing ion exchange across the plasma membrane and thus disrupting homeostasis. This phenomenon has given rise to promising strategies for the treatment of amyloid-derived diseases by the selective blocking of such ion channels (8–10). Therefore, the unfolding framework of PDZ3 described by Scheme 2 is extremely informative when it comes to obtaining experimental insight into the still poorly understood mechanism of amyloid formation and its resultant toxicity. The reversible coalescence under roughly physiological conditions of different kinds of well arranged supramacromolecular organizations during PDZ3 unfolding, together with the membrane-free organization of spherical/annular particulates, makes this protein system especially interesting for further studies into aggregation processes coupled to folding.

SUPPORTING MATERIAL

Methods and five figures are available at http://www.biophysj.org/biophysj/supplemental/S0006-3495(10)00434-0.

We thank Dr. J. Ruiz-Sanz and Dr. L. Bejarano for their helpful discussions and Dr. J. Trout for revising and correcting our English text. J.M.C. is a Spanish Government PhD fellow.

This work was supported by the Spanish Ministry of Science and Education (BIO2006-15517-C02-01/02, BIO2009-13261-C02-01/02), the Andalucian Regional Government (grant P09-CVI-5063 to A.C.A.), and the University of Granada (contract to E.S.C.).

REFERENCES

1. Feng, W., and M. Zhang. 2009. Organization and dynamics of PDZ-domain-related supramodules in the postsynaptic density. *Nat. Rev. Neurosci.* 10:87–99.
2. Jemth, P., and S. Gianni. 2007. PDZ domains: folding and binding. *Biochemistry.* 46:8701–8708.
3. Lockless, S. W., and R. Ranganathan. 1999. Evolutionarily conserved pathways of energetic connectivity in protein families. *Science.* 286:295–299.
4. Gianni, S., T. Walma, …, G. W. Vuister. 2006. Demonstration of long-range interactions in a PDZ domain by NMR, kinetics, and protein engineering. *Structure.* 14:1801–1809.
5. Petit, C. M., J. Zhang, …, A. L. Lee. 2009. Hidden dynamic allostery in a PDZ domain. *Proc. Natl. Acad. Sci. USA.* 106:18249–18254.
6. Sicorello, A., S. Torrassa, …, F. Chiti. 2009. Agitation and high ionic strength induce amyloidogenesis of a folded PDZ domain in native conditions. *Biophys. J.* 96:2289–2298.
7. Bucciantini, M., E. Giannoni, …, M. Stefani. 2002. Inherent toxicity of aggregates implies a common mechanism for protein misfolding diseases. *Nature.* 416:507–511.
8. Quist, A., I. Doudevski, …, R. Lal. 2005. Amyloid ion channels: a common structural link for protein-misfolding disease. *Proc. Natl. Acad. Sci. USA.* 102:10427–10432.
9. Shirwany, N. A., D. Payette, …, Q. Guo. 2007. The amyloid beta ion channel hypothesis of Alzheimer's disease. *Neuropsychiatr. Dis. Treat.* 3:597–612.
10. Jang, H., J. Zheng, …, R. Nussinov. 2008. New structures help the modeling of toxic amyloidbeta ion channels. *Trends Biochem. Sci.* 33:91–100.
11. Gianni, S., N. Calosci, …, C. Travaglini-Allocatelli. 2005. Kinetic folding mechanism of PDZ2 from PTP-BL. *Protein Eng. Des. Sel.* 18:389–395.
12. Feng, H., N. D. Vu, and Y. Bai. 2005. Detection of a hidden folding intermediate of the third domain of PDZ. *J. Mol. Biol.* 346:345–353.
13. Chi, C. N., S. Gianni, …, P. Jemth. 2007. A conserved folding mechanism for PDZ domains. *FEBS Lett.* 581:1109–1113.
14. Filimonov, V. V., and V. V. Rogov. 1996. Reversible association of the equilibrium unfolding intermediate of lambda Cro repressor. *J. Mol. Biol.* 255:767–777.

15. Ruiz-Sanz, J., V. V. Filimonov, …, P. L. Mateo. 2004. Thermodynamic analysis of the unfolding and stability of the dimeric DNA-binding protein HU from the hyperthermophilic eubacterium *Thermotoga maritima* and its E34D mutant. *Eur. J. Biochem.* 271:1497–1507.

16. Calamai, M., C. Canale, …, C. M. Dobson. 2005. Reversal of protein aggregation provides evidence for multiple aggregated states. *J. Mol. Biol.* 346:603–616.

17. Güthe, S., L. Kapinos, …, T. Kiefhaber. 2004. Very fast folding and association of a trimerization domain from bacteriophage T4 fibritin. *J. Mol. Biol.* 337:905–915.

18. Fernandez-Escamilla, A. M., F. Rousseau, …, L. Serrano. 2004. Prediction of sequence-dependent and mutational effects on the aggregation of peptides and proteins. *Nat. Biotechnol.* 22:1302–1306.

19. Cámara-Artigas, A., J. Murciano-Calles, …, J. C. Martínez. 2010. Novel conformational aspects of the third PDZ domain of the neuronal post-synaptic density-95 protein revealed from two 1.4A X-ray structures. *J. Struct. Biol.* 170:565–569.

20. Smith, A. M., T. R. Jahn, …, S. E. Radford. 2006. Direct observation of oligomeric species formed in the early stages of amyloid fibril formation using electrospray ionization mass spectrometry. *J. Mol. Biol.* 364:9–19.

21. Hawe, A., M. Sutter, and W. Jiskoot. 2008. Extrinsic fluorescent dyes as tools for protein characterization. *Pharm. Res.* 25:1487–1499.

22. Kad, N. M., S. L. Myers, …, N. H. Thomson. 2003. Hierarchical assembly of beta2-microglobulin amyloid in vitro revealed by atomic force microscopy. *J. Mol. Biol.* 330:785–797.

23. Kardos, J., K. Yamamoto, …, Y. Goto. 2004. Direct measurement of the thermodynamic parameters of amyloid formation by isothermal titration calorimetry. *J. Biol. Chem.* 279:55308–55314.

24. Morel, B., S. Casares, and F. Conejero-Lara. 2006. A single mutation induces amyloid aggregation in the alpha-spectrin SH3 domain: analysis of the early stages of fibril formation. *J. Mol. Biol.* 356:453–468.

25. Apetri, M. M., N. C. Maiti, …, V. E. Anderson. 2006. Secondary structure of alpha-synuclein oligomers: characterization by Raman and atomic force microscopy. *J. Mol. Biol.* 355:63–71.

26. Carrotta, R., M. Manno, …, P. L. San Biagio. 2005. Protofibril formation of amyloid beta-protein at low pH via a non-cooperative elongation mechanism. *J. Biol. Chem.* 280:30001–30008.

27. Juárez, J., P. Taboada, and V. Mosquera. 2009. Existence of different structural intermediates on the fibrillation pathway of human serum albumin. *Biophys. J.* 96:2353–2370.

28. Martínez, J. C., M. el Harrous, …, A. R. Fersht. 1994. A calorimetric study of the thermal stability of barnase and its interaction with 3′ GMP. *Biochemistry.* 33:3919–3926.

29. Calosci, N., C. N. Chi, …, P. Jemth. 2008. Comparison of successive transition states for folding reveals alternative early folding pathways of two homologous proteins. *Proc. Natl. Acad. Sci. USA.* 105:19241–19246.

30. Filimonov, V. V., J. Prieto, …, L. Serrano. 1993. Thermodynamic analysis of the chemotactic protein from *Escherichia coli*, CheY. *Biochemistry.* 32:12906–12921.

31. Kodali, R., and R. Wetzel. 2007. Polymorphism in the intermediates and products of amyloid assembly. *Curr. Opin. Struct. Biol.* 17:48–57.

32. Jiang, Y., H. Li, …, S. Perrett. 2004. Amyloid nucleation and hierarchical assembly of Ure2p fibrils. Role of asparagine/glutamine repeat and nonrepeat regions of the prion domains. *J. Biol. Chem.* 279:3361–3369.

33. Binger, K. J., C. L. Pham, …, G. J. Howlett. 2008. Apolipoprotein C-II amyloid fibrils assemble via a reversible pathway that includes fibril breaking and rejoining. *J. Mol. Biol.* 376:1116–1129.

34. Krebs, M. R., G. L. Devlin, and A. M. Donald. 2007. Protein particulates: another generic form of protein aggregation? *Biophys. J.* 92:1336–1342.

35. Walsh, P., J. Yau, …, S. Sharpe. 2009. Morphology and secondary structure of stable beta-oligomers formed by amyloid peptide PrP(106-126). *Biochemistry.* 48:5779–5781.

36. Serio, T. R., A. G. Cashikar, …, S. L. Lindquist. 2000. Nucleated conformational conversion and the replication of conformational information by a prion determinant. *Science.* 289:1317–1321.

37. Hoyer, W., T. Antony, …, V. Subramaniam. 2002. Dependence of alpha-synuclein aggregate morphology on solution conditions. *J. Mol. Biol.* 322:383–393.

38. Zheng, J., H. Jang, …, R. Nussinov. 2008. Annular structures as intermediates in fibril formation of Alzheimer Abeta17-42. *J. Phys. Chem. B.* 112:6856–6865.